Arabian Journal for Science and Engineering (2019) 44:1685–1696
https://doi.org/10.1007/s13369-018-3654-8

RESEARCH ARTICLE - MECHANICAL ENGINEERING

Investigation of Natural Convection Heat Transfer Along a Uniformly Heated Vertical Plate

Sebiha Yildiz[1] · **Burak Başaran**[1]

Received: 22 March 2018 / Accepted: 19 November 2018 / Published online: 1 December 2018

Abstract
Natural convection heat transfer along a vertical plate with uniform heat fluxes ranging from 400 to 1000 W m^{-2} was investigated by using air. The local surface temperatures on the heated surface were calculated by utilizing correlations existing in the literature. Computational analysis was also performed to determine the local wall temperatures for natural convection. The results of computational analysis of the velocity distribution of the fluid in the hydrodynamic boundary layer are presented as well as the thermal distribution in the velocity boundary layer, respectively. The local temperatures determined by those correlations were compared both with each other and then with the results of the computational analysis. The local temperature results obtained in the computational analysis were in good agreement with one of those correlations and demonstrate that the increase in uniform wall heat flux causes both an increase in the local wall temperature and an increase in the velocity of air in the hydrodynamic boundary layer. It was observed that local wall temperature had risen with the increase in the distance from the plate edge.

Keywords Natural convection · Uniform wall heat flux · A vertical plate · Air · Computational analysis

List of symbols

g	Gravity constant (m s^{-2})
Gr^*	Modified Grashof number (–)
h	Convection heat transfer coefficient (W $m^{-2}K^{-1}$)
k	Thermal conductivity (W $m^{-1}K^{-1}$)
Nu	Nusselt number (–)
P	Pressure (Pa)
Pr	Prandtl number (–)
$\dot{q}$	Heat flux (W m^{-2})
Ra	Rayleigh number (–)
Ra^*	Modified Rayleigh number (–)
T	Temperature (K)
u, v	Average fluid velocity components (m s^{-1})
x, y	Cartesian coordinates (m)

Greek symbols

α	Thermal diffusivity (m^2s^{-1})
β	Volumetric thermal expansion coefficient (K^{-1})
θ	Plate angle (°)
μ	Dynamic viscosity (kg $m^{-1}s^{-1}$)
υ	Kinematic viscosity (m^2s^{-1})
ρ	Mass density (kg m^{-3})

Subscripts

atm	Atmospheric
f	Film temperature conditions
in	Inlet
out	Outlet
w	Wall
y	Local
∞	Ambient conditions

✉ Sebiha Yildiz
syildiz@yildiz.edu.tr

Burak Başaran
basaranburak@outlook.com; burak.basaran@enka.com

[1] Department of Mechanical Engineering, Faculty of Mechanical Engineering, Yildiz Technical University, 34349 Istanbul, Turkey

1 Introduction

Natural convection is a mechanism by which fluid movement results from the density differences caused by the heating process. In this process, the heat reduces the density of the

fluid adjacent to the heated plate. The buoyant force is created by the density difference of the fluid. The buoyant force drives the fluid to move. This passive cooling method, which is commonly utilized in such devices as electronic equipment, PV modules, and the like, is both easy to deploy and does not require any external energy. However, because the temperature significantly influences the electrical efficiency and power output of many of these devices (both of which decrease with an increase in cell temperature), knowledge of the surface temperatures of such devices becomes critical (Dubey et al. [1], Mittelman et al. [2], Lee et al. [3]). Moreover, because uniform heat flux may cause the wall temperature of the device to exceed its melting point, there is also the possibility that the system itself might fail. It is only by knowing and maintaining the operating temperatures of these electronic devices at determined levels that such malfunctions and system failures can be prevented. The solution for these kinds of problems rests in the calculation and use of heat transfer coefficients. The correlations found in the published works discussed below can be used to determine the local heat transfer coefficient with distance from the plate edge:

Vliet [4] set up an experiment and used working fluid such as water and air to investigate the local heat transfer for natural convection on an inclined plate. His experiment employed a 1.22-m-high and 0.91-m-wide upward-facing, electrically heated, stainless steel plate that was insulated on its back face. The plate inclined 30°–90° from the horizontal. The heat flux ranged from 300 to 20×10^3 W m^{-2}, while the bulk water temperature was maintained near room temperature. The air was used at an inclination angle of 45° for the approximate heat fluxes of 300–550 W m^{-2} as a means of increasing the Prandtl number range. Vliet found that significant heat loss corrections, such as radiation to the surroundings and conduction through the insulated backing, were necessary for the air experiments. He proposed the following correlation for laminar natural convection with the gravity component which is parallel to the heated surface in Grashof number as follows:

$$Nu_{\mathrm{y}} = 0.60\left(Gr_{\mathrm{y}}^{*}Pr\right)^{0.2} \tag{1}$$

Here the local Nusselt number

$$Nu_{\mathrm{y}} = h_y y/k \tag{2}$$

and the local modified Grashof number

$$Gr_{\mathrm{y}}^{*} = \left(g\beta q_w y^4\right) / \left(k\nu^2\right) \tag{3}$$

are given. In this correlation, the gravity in Gr_{y}^{*} is replaced by the component parallel to the plate which is $g \sin\theta$, where θ is the angle from the horizontal. He evaluated the properties at the mean boundary-layer temperature and found that the inclination played a strong role in starting the turbulent regime. The value of $Gr_{\mathrm{y}}^{*}Pr$ for transition decreased from a mean value near 10^{13} for a vertical surface to approximately 10^8 for a surface inclination of 30° to the horizontal. He suggested the following correlation for turbulent natural convection for both vertical and inclined surfaces as follows:

$$Nu_{\mathrm{y}} = 0.30\left(Gr_{\mathrm{y}}^{*}Pr\right)^{0.24} \tag{4}$$

Vliet and Liu [5] utilized water as the working fluid in the experiment they conducted to investigate the turbulent natural convection throughout a uniformly heated vertical plane. Here, the researchers used a 0.91-m-wide and 1.22-m-high electrically heated, stainless steel plate. Their focus on the turbulent region allowed them to gather laminar, transitional and turbulent natural convection local heat transfer data. This experiment led them to conclude that the correlation derived from this [4] study bears close correspondence to all of the previously obtained laminar natural convection data. Their results indicate that the natural transition appears within the range $10^{12} < Gr_{\mathrm{y}}^{*}Pr < 10^{14}$, which means that a fully developed turbulent flow presents itself at $Gr_{\mathrm{y}}^{*}Pr = 10^{14}$. The turbulent heat transfer data for $Gr_{\mathrm{y}}^{*}Pr$ rose to as high as 10^{16}. They also conclude that the following equation represents a good correlation of all of the turbulent data from the vertical and inclined surfaces:

$$Nu_{\mathrm{y}} = 0.568\left(Gr_{\mathrm{y}}^{*}Pr\right)^{0.22} \tag{5}$$

Vliet and Ross [6] conducted an experimental study. In this work the researchers used air as the working fluid to investigate the local heat transfer for turbulent natural convection on vertical plate, inclined upward and downward. In this study, the researchers used metal foil to heat a 1.83-m-wide and 7.32-m-high test plate and a heat flux ranging from 26 to 97 W m^{-2}. These air-based experiments were performed for modified Grashof numbers up to 10^{15}. They measured the local surface temperatures along the uniformly heated plate at inclinations ranging from 30° from the vertical (upward facing—unstable) to 80° from the vertical (downward facing—stable). They demonstrated that the angle of the plate affects the transition heat transfer. The authors reported that in some cases the laminar flow stops when the temperature of the plate either no longer increases or reaches a weak maximum. They also reported that a fully turbulent flow begins where the plate temperature becomes constant. The transition range occurs between laminar and turbulent locations. In the unstable case, when the vertical angle of the plate increases, the length decreases where the transition starts. In contrast, in the stable case, when the vertical angle of plate increases, the length increases where the transition starts; the increase in heat flux also causes a decrease in the length of the position of transition. The following correlation

by Dotson [7], which was cited in Vliet and Ross [6], is for laminar data of both orientations:

$$Nu_y = 0.55\left(Gr_y^* Pr\right)^{0.20} \tag{6}$$

in which the gravitational acceleration throughout the plate is $g\cos\theta$ where θ is measured from the vertical. Vliet and Ross also suggested the following equation which includes the turbulent natural convection data:

$$Nu_y = 0.17\left(Gr_y^* Pr\right)^{0.25} \tag{7}$$

For the unstable case, the correlation for the turbulent natural convection does not include the angle of the plate, whereas for the stable case g is replaced by $g\cos^2\theta$.

Based on the solutions of the boundary layers for free convection on a uniformly heated vertical plate in the literature, Fujii and Fujii [8] expressed the local Nusselt number as:

$$Nu_y = C^*\left(Gr_y^* Pr\right)^{1/5} \tag{8}$$

where the values of C^* are a function of Pr as follows:

$$C^{*5} = Pr/(4 + 9Pr^{1/2} + 10Pr) \tag{9}$$

which is valid for any range of Prandtl numbers.

Churchill and Ozoe [9] proposed the following equation, which can be used for all Prandtl numbers for the natural convection for laminar flow from a uniformly heated vertical plate:

$$Nu_y = 0.563Ra_y^{1/4}\Big/\left[1 + (0.437/Pr)^{9/16}\right]^{4/9} \tag{10}$$

This equation was derived from an asymptotic solution for boundary-layer equations. For Eq. (10), the Nusselt number and local Rayleigh number are given as follows:

$$Nu_y = q_w y/k\left(T_y - T_\infty\right) \tag{11}$$

and

$$Ra_y = g\beta\left(T_y - T_\infty\right)y^3/\nu\alpha \tag{12}$$

They suggested that Eqs. (10), (11) and (12) can be used to obtain T_y.

In their work, Aydın and Guessous [10] put forth dimensional arguments to find a dimensionless number for the correlations of the heat transfer in natural convection along the plate with the uniform heat flux for both the laminar and the turbulent regimes. The dimensionless number is given as follows:

$$\Pi_Q = \frac{Ra^* Pr}{C_0 + Pr} \tag{13}$$

The heat transfer for laminar and for the turbulent flow was introduced in the form of $Nu \sim \Pi_Q^{1/5}$ and $Nu \sim \Pi_Q^{1/4}$, respectively.

In their work, Kobus et al. [11] used an integral technique to develop the correlations for the natural convection of laminar flow on a vertical plate using constant heat flux. The dimensionless group obtained by these researchers is similar to the correlation proposed by Aydın and Guessous [10]. Kobus et al. [11]'s integral model is:

$$\frac{Nu_y}{Gr_y^{*1/5}} = C_1\left(\frac{Pr^2}{C_0 + Pr}\right)^{1/5} \tag{14}$$

where the constants C_0 and C_1 depend on the temperature profile. Similar to the conclusions put forth by Aydın and Guessous [10], the correlations provided by Kobus et al. [11] are also valid for large ranges of the Prandtl number.

It is known that practical problems involving fluid dynamics and heat transfer are more readily solved by using computational analysis (CA), which proves useful in predicting laminar and turbulent flows. Laein et al. [12] carried out particle image velocimetry (PIV) on the nanofluid free convection at vertical and horizontal plates used constant heat flux. They investigated the flow boundary layer and compared their experimental findings with the computational analysis. Their efforts to develop some theoretical methods led them to conclude that the velocity of flow around the plate increases parallel to the increase in wall heat flux.

Fahiminia et al. [13] carried out a computational analysis to determine the natural convection heat transfer on the heated vertical surfaces in air. To do this, they set a model of a heat sink having vertical rectangular fins placed in regular intervals. They reported that their numerical model allowed them to precisely predict the air flow of natural convection around the heat sink.

Saha et al. [14] carried out both an improved mathematical analysis and direct numerical simulations for an inclined plate with uniform heat flux. In their work they developed a modified Prandtl number scaling which uses a triple-layer integral approach for $Pr > 1$. To develop a numerical model, Teymourtash et al. [15] analyzed the natural convection of supercritical fluids along a vertical plate with constant and variable heat fluxes. In his work Pantokratoras [16] investigated the steady laminar boundary layer flow by using glycerol along a uniformly heated vertical plate and used his findings to develop boundary layer equations numerically for both upward and downward flows. Zitzmann et al. [17] carried out free convection over a heated vertical plate

and focused their investigation on the influence of near-wall mesh density on air flow and free convection heat transfer.

Khan and Aziz [18] used a combined similarity-numerical approach in the natural convective boundary layer using nanofluid along a vertical plate which had a uniform heat flux. They carried out a regression analysis to obtain correlations for the Nusselt number. Perovic et al. [19] studied the inclination angle's effect on natural convection over the photovoltaic module. These researchers developed a group of new correlations for the isothermal plate based on the existing experimental and numerical results in the literature. Guha et al. [20] focused their attention on the production of a unified integral theory that could be used to determine the laminar natural convection on an inclined surface and to determine the variation in surface temperature and surface heat flux. To this end, they developed new algebraic correlations where the Nusselt number was given as functions of inclination angle, Prandtl number and Grashof number.

To date most of the studies available in the literature for air have been performed at low wall heat fluxes. This study will, therefore, contribute to the existing literature in that it deals with heat transfer by natural convection for air along a vertical plate with relatively higher heat fluxes.

Despite all of the work conducted thus far and even though it is a known fact that many devices operate with uniform wall heat flux, a limited number of studies have focused on this precise issue, opening up the necessity of examining natural convection on a uniformly heated plate. The uniform wall heat flux is a critical requirement, for if we can predict the wall temperature of these devices, we will be better able to control the temperature, thus preventing system failures and ensuring efficient use of these kinds of devices. The control need of device temperature leads us to focus on the study of the local wall temperatures in natural convection of air over a vertical flat plate with different heat fluxes. In the presented study, the local wall temperatures of uniformly heated vertical plates were determined using both the existing correlations in the literature and computational analysis.

2 Determining Local Surface Temperatures with Existing Correlations

In order to determine local wall temperatures, a trial-and-error method was used via the correlations proposed by Vliet [4], Fujii and Fujii [8] and Churchill and Ozoe [9] for each of the 0.1 m distances from the bottom edge of the center line of the vertical plate for each of the given uniform heat fluxes. Since the surface temperature is not known, the surface temperature must be estimated to determine T_f and the air properties accordingly. To achieve this, this iterative solution must begin with an estimated value of the local heat transfer coefficient (h_y) for Vliet [4] and Fujii and Fujii [8] and with an estimated value of the local surface temperature (T_y) for Churchil and Ozoe [9]. If the local heat transfer coefficient is taken as this estimated value, the approximate temperature difference between the wall and the ambient is obtained as follows:

$$T_y - T_\infty = \dot{q}_w / h_y \tag{15}$$

where $\dot{q}_w$ is the uniform heat flux at the plate, h_y is the estimated value of the local convection coefficient, T_∞ is the ambient temperature, and T_y is the local surface temperature at a given distance.

Then, the film temperature can be calculated as

$$T_f = \frac{(T_y - T_\infty)}{2} + T_\infty \tag{16}$$

and at T_f, the air properties can be evaluated.

From Eq. (3) the modified Grashof number is determined where β is the volume expansion coefficient for air as an ideal gas as follows:

$$\beta = \frac{1}{T_f} \tag{17}$$

The modified Rayleigh number is the product of the modified Grashof and Prandtl numbers as follows:

$$Ra_y^* = \left(Gr_y^* Pr\right) \tag{18}$$

where Prandtl number

$$Pr = \nu/\alpha \tag{19}$$

Then the correlations by Vliet [4] and Fujii and Fujii [8] were used to calculate h_y. The same method was also applied to the correlation proposed by Churchill and Ozoe [9], but the estimated value was the local wall temperature.

Vliet [4] suggested that the beginning of the transition from laminar to turbulent for a vertical heated surface occurs at approximately the Rayleigh number of 10^{13}. In this study, we used the maximum calculated Rayleigh number of 10^{11} which is lower than the value mentioned in Vliet's study. Therefore, Eq. (1) proposed by Vliet [4] was used for laminar flow.

3 Governing Equations

This study considered a steady two-dimensional natural convection air flow along a uniformly heated vertical flat surface. Figure 1 shows the flow configuration where x measures the horizontal distance from the surface in the direction normal to y. The gravity force acts in the negative y direction. The

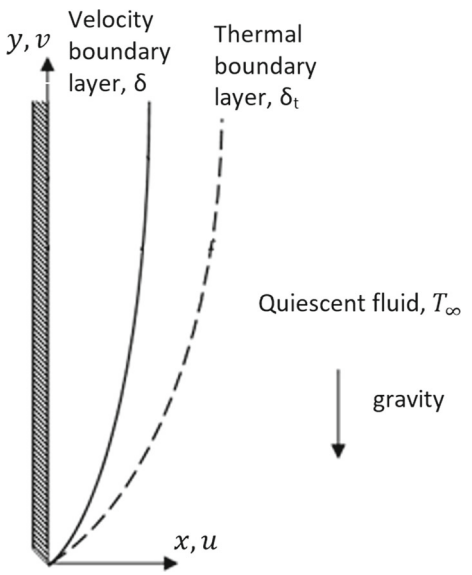

Fig. 1 Sketch of the boundary layers in natural convection for $Pr < 1$

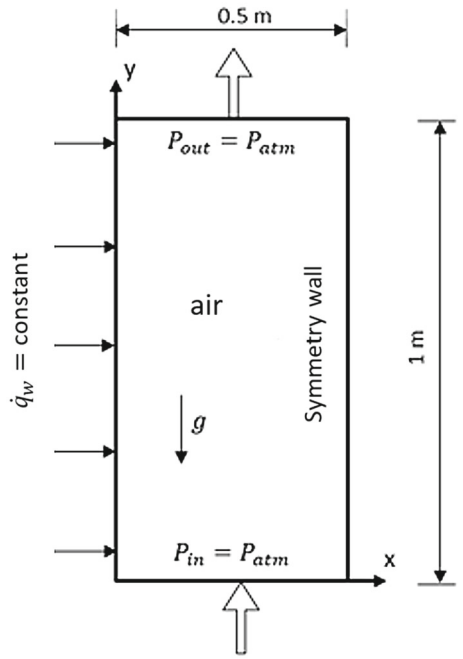

Fig. 2 Sketch of the computational domain

ambient temperature T_∞ is taken as constant. Here, u and v are the x- and y- components of the fluid velocity.

The governing equations represent the conservation of mass, momentum and energy in [21] as follows:

Mass conservation

$$\frac{\partial u}{\partial x} + \frac{\partial u}{\partial y} = 0 \tag{20}$$

x-Momentum conservation

$$\rho\left(u\frac{\partial u}{\partial x} + v\frac{\partial u}{\partial y}\right) = -\frac{\partial P}{\partial x} + \mu\left(\frac{\partial^2 u}{\partial x^2} + \frac{\partial^2 u}{\partial y^2}\right) \tag{21}$$

y-Momentum conservation

$$\rho\left(u\frac{\partial v}{\partial x} + v\frac{\partial v}{\partial y}\right) = -\frac{\partial P}{\partial y} + \mu\left(\frac{\partial^2 v}{\partial x^2} + \frac{\partial^2 v}{\partial y^2}\right) - \rho g \tag{22}$$

Energy conservation

$$u\frac{\partial T}{\partial x} + v\frac{\partial T}{\partial y} = \alpha\left(\frac{\partial^2 T}{\partial x^2} + \frac{\partial^2 T}{\partial y^2}\right) \tag{23}$$

Equation (21) can be reduced to:

$$\frac{\partial P}{\partial x} = 0 \quad \text{since} \quad u \ll v \tag{24}$$

The transversal momentum Eq. (21) reduces to the statement that the pressure in the boundary layer is a function of longitudinal position

$$\frac{\partial P}{\partial y} = \frac{\mathrm{d}P}{\mathrm{d}y} = \frac{\mathrm{d}P_\infty}{\mathrm{d}y} = -\rho_\infty g \tag{25}$$

The momentum Eq. (22) becomes

$$\rho\left(u\frac{\partial v}{\partial x} + v\frac{\partial v}{\partial y}\right) = g(\rho_\infty - \rho) + \mu\left(\frac{\partial^2 v}{\partial x^2} + \frac{\partial^2 v}{\partial y^2}\right) \tag{26}$$

The density field $\rho(x, y)$ drives the flow generated by the temperature field $T(x, y)$. The numerical studies cited in the literature demonstrate that most natural convection problems have been solved under the Boussinesq approximation. However, the Boussinesq approximation is valid only for low temperature differences and considers all physical properties constant, except in the buoyancy force (Bouafia et al. [22], Huang et al. [23]). The significant difference between plate surface temperature and ambient temperature in this study led us, therefore, to apply the ideal gas approximation. The density of air was calculated via the ideal gas law,

$$\rho = P/RT \tag{27}$$

The boundary conditions taken for a uniformly heated vertical plate are as follows

$$at\ x = 0, u = v = 0, \dot{q}_w = -k\frac{\partial T}{\partial x} + \dot{q}_r \tag{28}$$

$$as\ x \to \infty, u = v = 0, T = T_\infty \tag{29}$$

where the uniform heat flux at the plate is $\dot{q}_w$, the radiation heat lost is $\dot{q}_r$, and the ambient temperature is T_∞. In order to determine u, v and T in the boundary layer, Eqs. (20)–(27) are solved with the boundary conditions in Eqs. (28) and (29). From these equations, the temperature field $T(x, y)$ needs determining for the uniform surface heat flux.

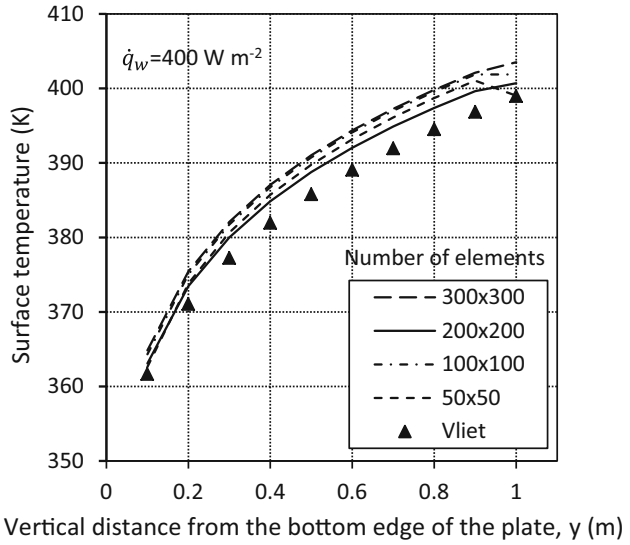

(a)

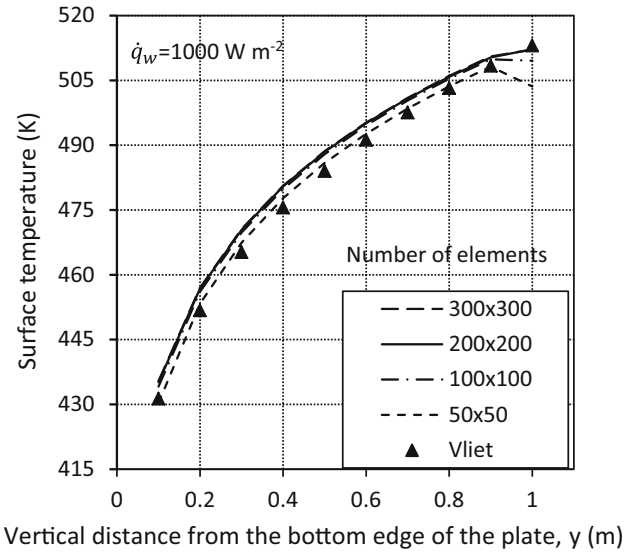

(b)

Fig. 3 Comparison of the surface temperatures proposed by Vliet with those of computational analysis with radiation heat loss for a different number of elements **a** for the heat flux of 400 W m^{-2}; **b** for the heat flux of 1000 W m^{-2}

4 Computational Analysis

The commercial code FLUENT 6.0 was deployed in the computational analyses (CA) for the numerical solution of the governing Eqs. (20)–(27). During the modeling of the boundary layer over a vertical rectangular plate under natural convection conditions, the governing equations were assumed as steady, laminar, incompressible and two-dimensional. Semi-implicit and second-order upwind methods were used in solving the governing equations. The absolute criterion was

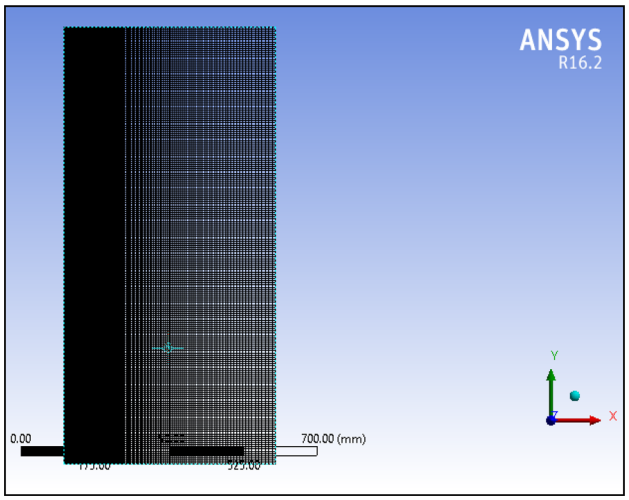

Fig. 4 Computational grid for the number of elements of 200 × 200

chosen as 10^{-5} under the residual monitors for the highest accuracy.

For the conversion of the governing equations into algebraic equations, FLUENT deploys a control-volume-based technique where the region in which the flow will be solved is subdivided into individual cells or control volumes, thus allowing the equations to be integrated numerically on a cell-by-cell basis, which produces discrete algebraic (finite volume) equations. The variables such as velocity components, pressure and temperature are applied to a control volume in mean values. The convective fluxes are evaluated using the control volume face values of the dependent variables. FLUENT's segregated steady-state solver is applied in the numerical simulations. Pressure and velocity are input values for the SIMPLE algorithm. In the application of simulations, the space discretization of the momentum and energy equations is made using a second-order upwind scheme. Also, in the momentum equations, to interpolate the pressure value and density on the control volume faces from those at the control volume centers, an accurate second-order scheme was chosen.

The plate used was 1 m in height and 1 m in width. The plate was assumed to be aluminum with an emissivity of 0.05 and to be insulated on its back face. The uniform heat fluxes on the surface were 400, 600, 800 and 1000 W m^{-2}. Vliet [4] reported that in the air experiment he carried out, it had become necessary to perform significant heat loss corrections (radiation and back conduction). This study carried out the computational analysis both with and without radiation heat loss. In this study, surface-to-surface model was taken into consideration for the radiation heat loss from the heated surface. Note that the right wall of the domain in Fig. 2 is the symmetrical wall.

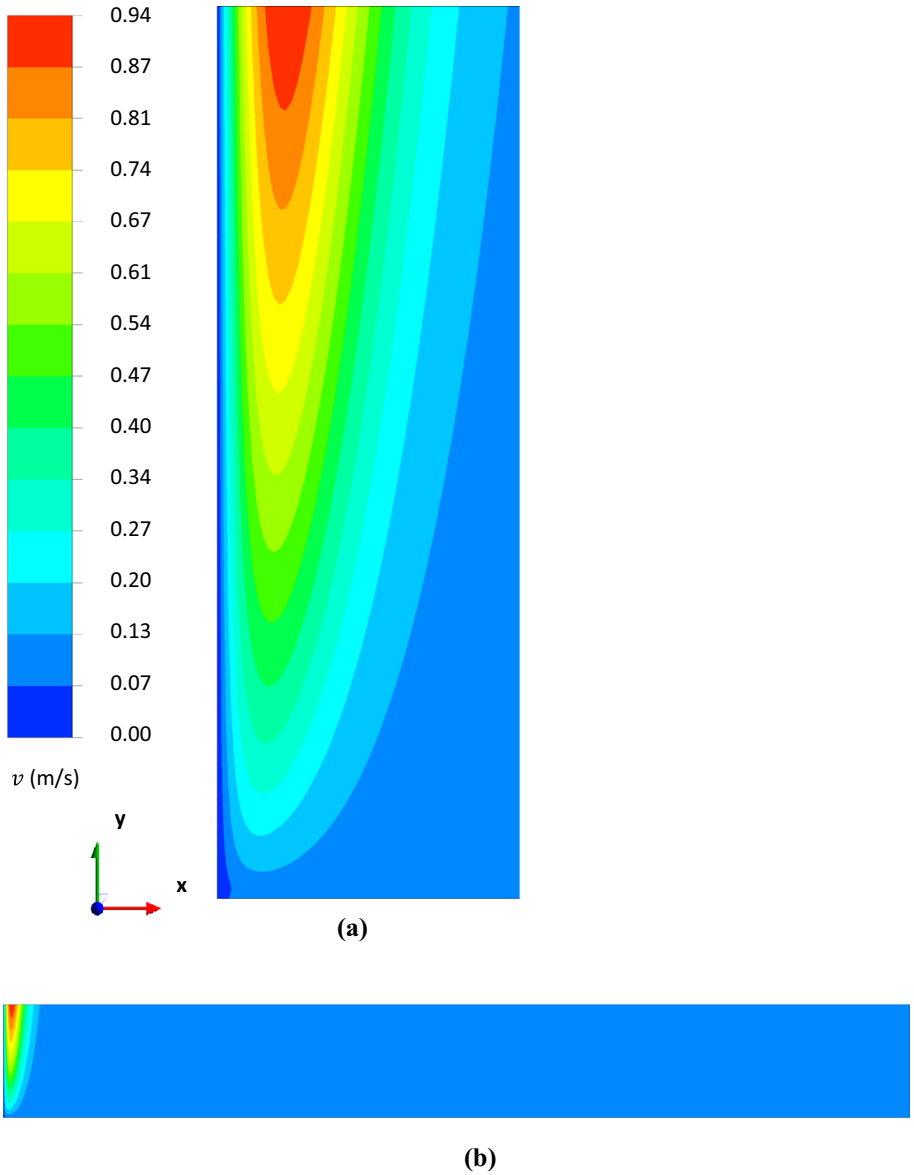

Fig. 5 Velocity contour showing the dynamic boundary layer along the vertical plate for the heat flux of 400 W m^{-2}: **a** close to the plate surface; **b** entire the domain

4.1 Boundary Conditions

The coordinate system was selected in such a way that y is measured along the plate and x measured perpendicular to the plate, respectively. The bottom leading edge of the heated plate's centerline was located in the origin of the coordinate system in Fig. 2. The temperature of the quiescent ambient air T_∞ is constant when it is distant from the plate. The entire surface of the plate is fixed at a constant heat flux. For the following domain in Fig. 2, the left wall is considered to be a hot wall maintained at a given uniform heat flux, and the right wall is considered as a symmetry wall maintained at the surrounding temperature T_∞. The other two walls (the top and bottom walls) are considered outlet and inlet pressure at atmospheric conditions. Even though it is a closed domain, the symmetry wall parallel to the plate is very far from the heated plate, and therefore, the closed domain does not have an important effect on the results inside the boundary layer due to the thickness of the thermal or viscous layer.

At this point, it is assumed that the fluid velocity at all fluid–solid boundaries is equal to that of the solid boundary, i.e., no-slip condition. The fluid temperature at all fluid–solid boundaries is equal to that of the solid boundary wall temperature, i.e., no jump condition. The air–fluid was quiescent outside of the velocity boundary layer.

4.2 Mesh Analysis

Engineering simulations involve the creation of an appropriate mesh that proves an accurate solution while also being effective in time reductions. In this study, mesh analyses were

performed in the number of elements of 50×50, 100×100, 200×200 and 300×300 for the uniform heat fluxes of 400 and 1000 W m^{-2}. As shown in Fig. 4, a non-uniform mesh is refined at the wall used near the vertical uniformly heated wall. Bias factor was chosen as 25.

The local wall temperatures along the center line of the heated plate were determined using computational analysis. In section 'Comparison of the results' of this paper, Fig. 12 displays both the local wall temperatures determined by using the Vliet [4], Fujii and Fujii [8] and Churchil and Ozoe [9] correlations and the results of the computational analysis. Figure 12 also shows that the results of the computational analysis including radiation heat loss are in better agreement with the results obtained by Vliet [4]. In light of this, Fig. 3 provides a comparison of all the mesh results for the number of elements of 50×50, 100×100, 200×200 and 300×300 for the wall heat fluxes of 400 and 1000 W m^{-2} with those of Vliet correlations. The ambient temperature was 300 K.

Some differences were noted between the results of all the number of elements and the correlation in use for the heat flux of 400 W m^{-2}. The local wall temperatures of the number of elements of 200×200 are closer to the results obtained by Vliet [4] than the results of the number of elements of 50×50, 100×100 and 300×300 (Fig. 3a). The maximum temperature difference between the results for the number of elements of 200×200 and the results according to Vliet [4] is 2.97 K, whereas this maximum difference for the results of the number of elements of 300×300 is 5.31 K. For the heat flux of 1000 W m^{-2}, the maximum temperature difference between the results of the number of elements of 200×200 and the results of Vliet' correlation is 5.18 K. The number of elements of 300×300 demonstrates a 5.36 K maximum temperature difference with Vliet's correlation (Fig. 3b).

As the difference in operating time between the number of elements of 200×200 and 300×300 was not significant, the fine number of elements of 200×200 was adopted for all of the following results. Figure 4 shows the domain for the number of elements of 200×200.

5 Results of Computational Analysis

Because heat transfer causes the fluid flow in the natural convection problem, thermal and hydrodynamic problems cannot be separated. A natural convection flow occurs as uniform heating is applied on the vertical plate. The plate is in a quiescent air fluid, and, with $T_y > T_\infty$, the density of the fluid near the plate is less than in the quiescent air. Buoyancy forces, therefore, induce a natural convection boundary layer in which the heated fluid rises vertically and entrains fluid from the quiescent region. A formation of the laminar boundary layer starts at the beginning of the leading edge of

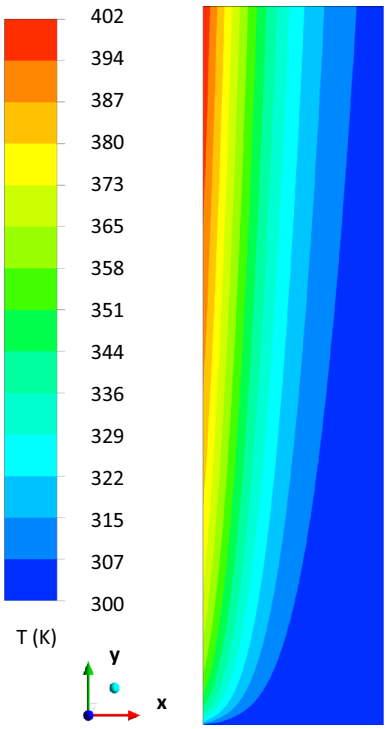

Fig. 6 Temperature contour showing thermal boundary growth along the central line of vertical plate for the heat flux of 400 W m^{-2}

the heated plate. The thickness of the layer increases along the direction of flow.

The results of computational analysis with radiation heat loss for local velocities and local temperatures were obtained for every 0.1 m on the vertical center line of the plate.

Figures 5, 6, 7 and 8 show the velocity and temperature contours for the heat fluxes of 400 and 1000 W m^{-2} using the number of elements of 200×200, respectively. Due to the non-slip nature of the boundary condition of the plate, the velocity of the fluid on the plate surface is zero. Move away from the wall horizontally, the velocity v gradually grows to a maximum under the effect of viscous friction in the boundary layer. Due to entraining fluid from the quiescent region, the air velocity beyond the dynamic boundary layer was almost 0.1 m s^{-1}. This situation can be seen in the entire domain for the heat flux of 400 W m^{-2} and on the bottom side of the domain for the heat flux of 1000 W m^{-2} in Figs. 5, 7, respectively.

Figures 6, 8 show the temperature counters for 400 and 1000 W m^{-2}, respectively. The air temperature at the heated wall increases with increasing vertical location for given heat flux. At the bottom of the plate, the local temperature was low for all of the heat fluxes because the air temperature is lower at the bottom of the wall. As a result, the convective heat transfer coefficient is high. As the vertical distance from the bottom increases, the temperature of air increases in the vicinity of the wall and hence the convective heat transfer

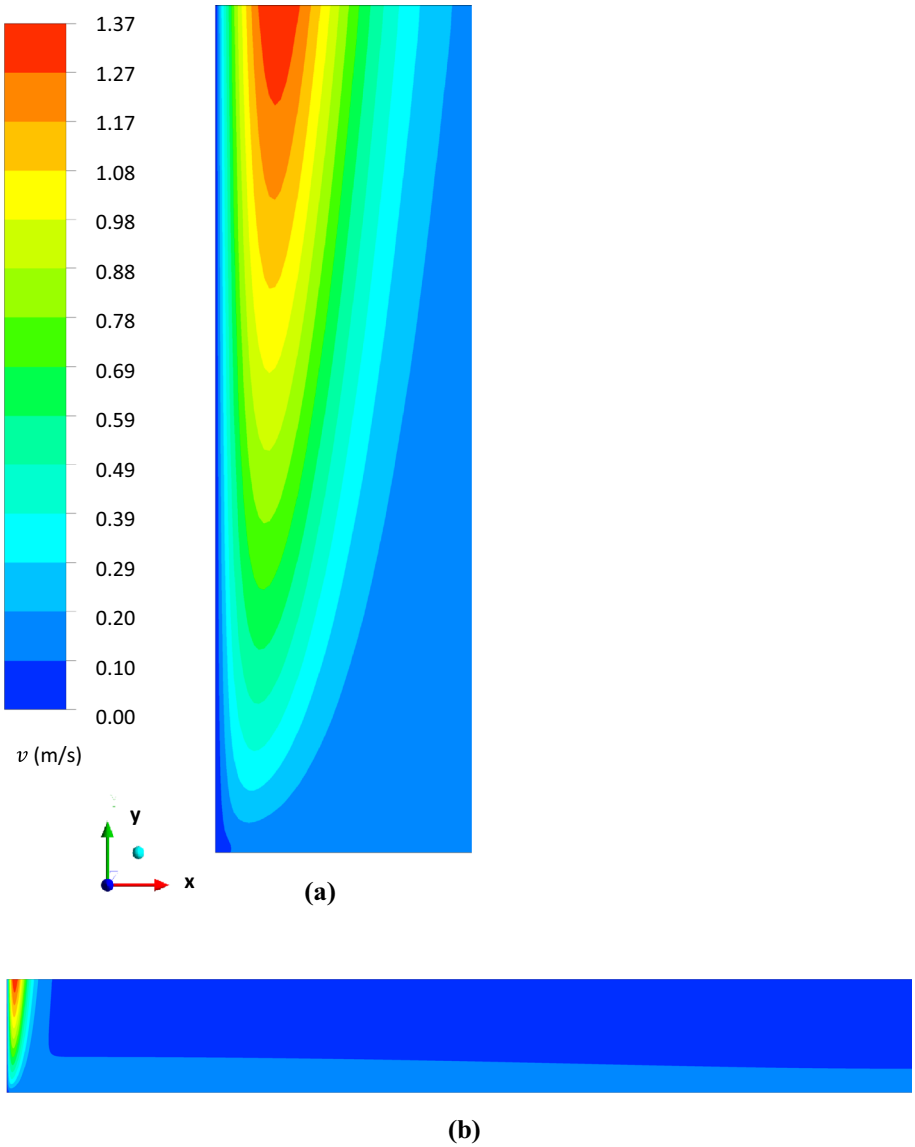

Fig. 7 Velocity contour showing the dynamic boundary layer along the vertical plate for the heat flux of 1000 W m^{-2}: **a** close to the plate surface; **b** entire the domain

coefficient decreases, resulting in a higher wall temperature. The temperature of air along the heated wall increases with the increase in the wall heat flux. Beyond the thermal boundary layer, the air temperature in the domain is equal to the surrounding temperature which was assumed as 300 K, as shown in Figs. 6, 8.

Figures 9, 10 show the local velocity profile and temperature profile of air in the layer of boundary on the heated plate. Figures 9a, 10a show the tendency of the velocity profiles of each of the heat fluxes along the heated plate to almost overlap onto a single line that extends beyond the dynamic boundary layer where the magnitude of the air velocity is about 0.1 m s^{-1}. The air temperature near the wall increases with an increasing axial location. The air flows contact the hot plate surface as it flows upward from the lower end of the heated plate. As this occurs, there is a heat transfer into the air from this heated plate and finally the air temperature increases along the plate. The air temperature at the top of the heated plate reaches a maximum, and the air velocity in the boundary layer reaches high values. The local temperature of air along the heated wall also increases with the increase in the heat flux. As evident in Figs. 9b, 10b, the temperature profiles for each of the heat fluxes overlap onto a single line when distant from the plate, where it is equal to the ambient temperature of 300 K.

Figure 11a, b shows the velocity profiles and the temperature profiles on the top of the uniformly heated vertical plate ($y = 1$ m) for the wall heat fluxes of 400, 600, 800, and 1000 W m^{-2}. The air flow velocity around the surface increases proportionally to wall heat flux. An increase in the heat flux yields a rise in temperature and a difference in density, which cause the fluid to flow more rapidly. As shown in Fig. 11a, the maximum air velocity rises with an increase in the wall heat flux. For the heat flux of 400 W m^{-2}, the

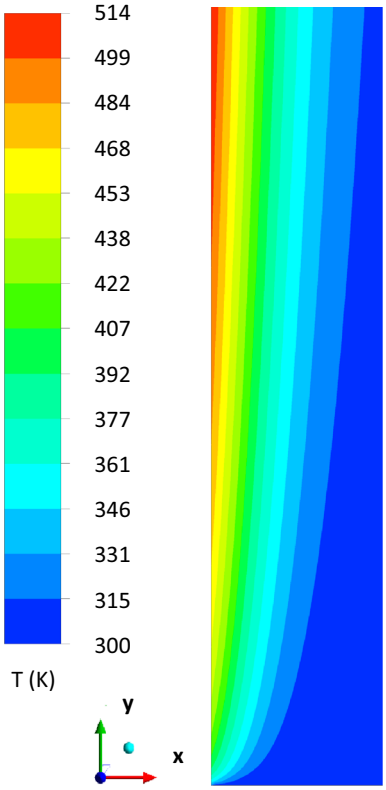

Fig. 8 Temperature contour showing thermal boundary growth along the central line of vertical plate for the heat flux of 1000 W m^{-2}

maximum air velocity was about 0.94 m s^{-1}, whereas for 1000W m^{-2}, it was about 1.37 m s^{-1}. The maximum temperature occurs at the top of the plate and is equal to 400.73 K for a heat flux of 400 W m^{-2} and 512.19 K for a heat flux of 1000 W m^{-2}.

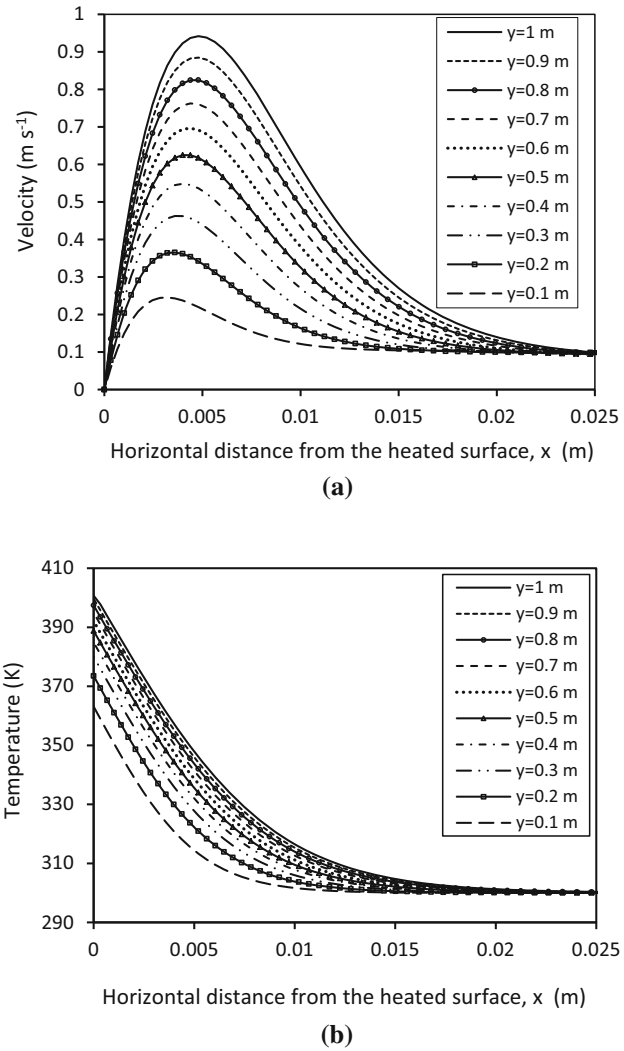

Fig. 9 **a** The velocity and **b** temperature profiles along the line perpendicular to the plate of the vertical central line for the heat flux of 400 W m^{-2}

6 Comparison of the Results

The results of the computational analysis for the uniform heat fluxes of 400 and 1000 W m^{-2} were compared to the local temperatures according to the correlations proposed by Vliet [4], Fujii and Fujii [8] and Churchil and Ozoe [9]. The results of the computational analysis are shown in Fig. 12, both with and without radiation heat loss.

All of the local wall temperatures increased with an increase in the distance from the edge with a relation of $y^1/5$. In addition to this, the increment of the wall heat flux caused to increase the local wall temperatures. The highest surface temperature occurred at the top of the vertical plate. The results of Fujii and Fujii [8] and Churchill and Ozone [9] are in agreement with each other, and the results of both studies overlap almost onto a single line. The local wall temperatures according to Fujii and Fujii [8] and Churchil and Ozoe [9] generally show the same tendency as shown in the results of computational analysis without radiation heat loss but with higher values. Churchil and Ozoe [9] reported that they solved the governing equations under the Boussinesq approximation under low temperature differences. However, because the temperature differences between the plate surface and ambient are higher than usual in this study, the Boussinesq approximation is not valid, so that the ideal gas approximation was applied. Therefore, the results from Churchil and Ozoe [9] may be different from the results of this study without the consideration of heat loss through radiation.

In general, the results of the computational analysis with radiation heat loss are in good agreement with those of Vliet [4] for all of the heat fluxes, as shown in Fig. 12. The surface temperatures for both computational analyses with radiation

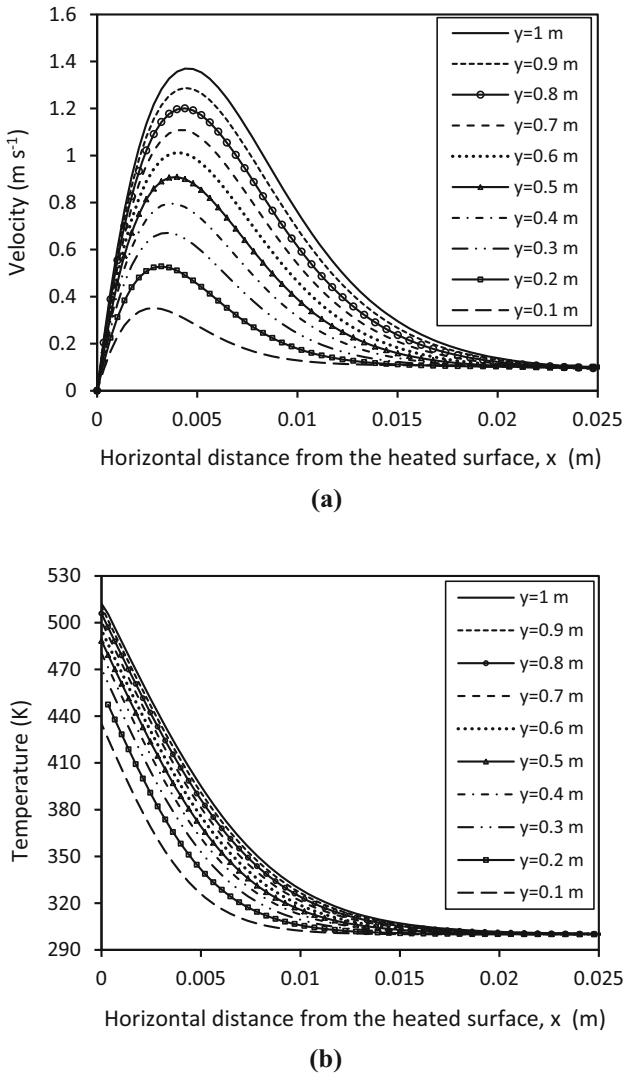

Fig. 10 **a** The velocity and **b** temperature profiles along the line perpendicular to the plate of the vertical central line for the heat flux of 1000 W m^{-2}

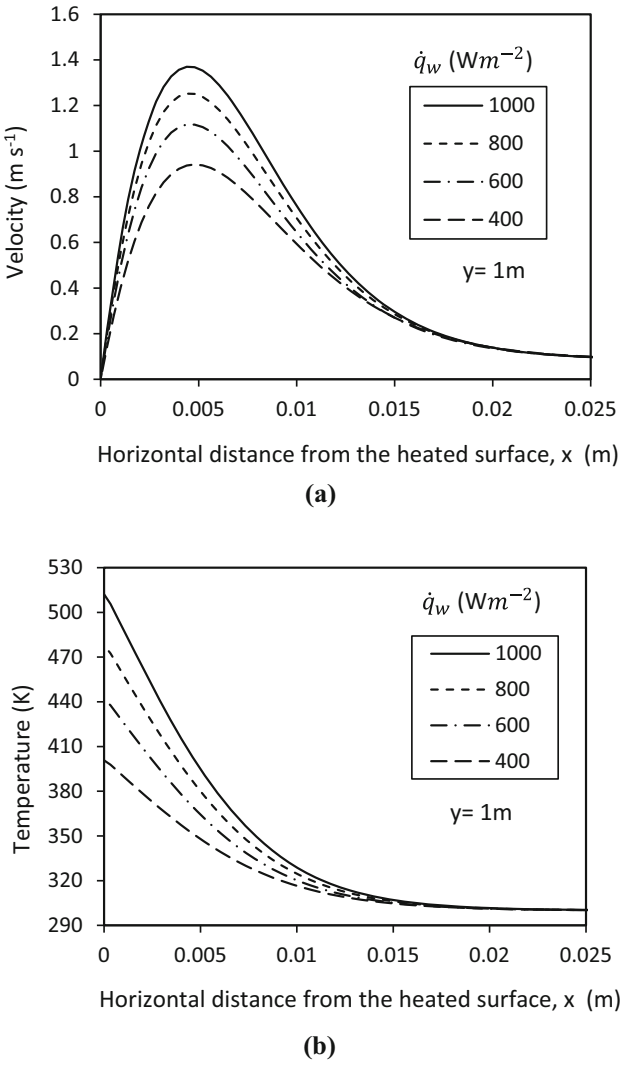

Fig. 11 Effects of the heat flux on the velocity and the temperature profile on the top of the plate

heat loss and Vliet [4] were lower than the temperatures obtained by Fujii and Fujii [8] and Churchil and Ozoe [9].

In the computational analysis if the heat loss caused by radiation is included, heat radiates directly from the walls into the environment and increment of air temperature next to the wall is less. Otherwise, air temperature will be high. Consequently, the effect of radiation on reducing the plate temperature is significant. The maximum temperature of the top wall is 512.19 K including radiation and 530.88 K without radiation for the heat flux of 1000 W m^{-2}. The heat fluxes lost by radiation with the emissivity of 0.05 were estimated 5% for the wall heat flux of 400 W m^{-2} and 6.5% for the wall heat flux of 1000 W m^{-2}. In conclusion, as can be seen in Fig. 12, the results of the computational analysis with radiation heat loss and the results of Vliet [4]'s correlation are in good agreement.

7 Conclusion

The natural convection heat transfer was investigated to determine the local wall temperatures along the centerline of a vertical uniformly heated plate. The correlations proposed by Vliet [4], Fujii and Fujii [8] and Churchil and Ozoe [9] and computational analysis were both used in this study to obtain the local wall temperatures. Two-dimensional computational analyses were performed to determine the local wall temperatures on a vertical uniformly heated plate using the heat fluxes of 400, 600, 800 and 1000 W m^{-2} with the number of elements of 200×200. This study demonstrates that the incremental distance from the plate' edge is an important parameter as it significantly affects the local wall temperatures. Another important parameter is the magnitude of the heat flux. Consequently, the larger the heat flux, the higher the

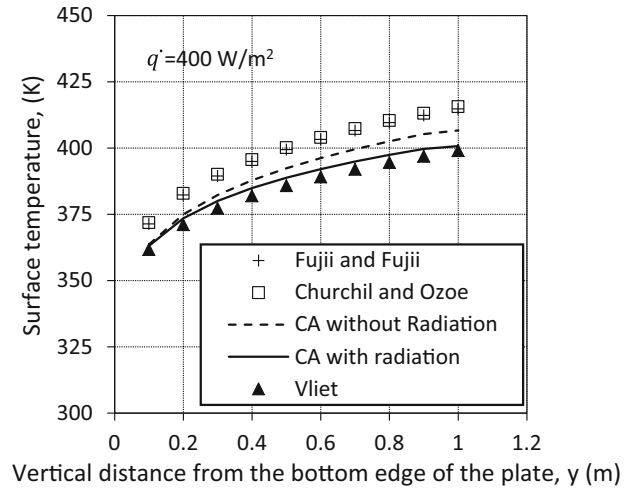

Fig. 12 Comparison of the local wall temperatures according to correlations with the results of computation analysis for different surface heat fluxes along the vertical plate

surface temperature, as predicted. Increment in the uniform wall heat flux causes an increase in the velocity around the plate. Generally, in case of taking into consideration of radiation heat loss in the computational analysis, the results are in good agreement with the results of Vliet [4]'correlation.

The above findings can be applied to the prediction of wall temperatures on electronic equipment having uniform heat flux.

References

1. Dubey, S.; Sarvaiya, J.N.; Seshadri, B.: Temperature dependent photovoltaic (PV) efficiency and its effect on PV production in the word-a review. Energy Procedia **33**, 311–321 (2013)
2. Mittelman, G.; Alshare, A.; Davidson, J.H.: A model and heat transfer correlation for rooftop integrated photovoltaics with a passive air cooling channel. Solar Energy **83**, 1150–1160 (2009)
3. Lee, Y.; Taya, A.A.O.: Finite element thermal analysis of a solar photovoltaic modüle. Energy Procedia **15**, 413–420 (2012)
4. Vliet, G.C.: Natural convection local heat transfer on constant-heat-flux inclined surface. J. Heat Transf. **91**(4), 511–517 (1969)
5. Vliet, G.C.; Liu, C.K.: An experimental study of turbulent natural convection boundary layers. J. Heat Transf. **91**(4), 517–531 (1969)
6. Vliet, G.C.; Ross, D.C.: Turbulent natural convection on upward and downward facing inclined constant heat flux surfaces. J. Heat Transf. **97**(4), 549–554 (1975)
7. Dotson, J.P.: Heat transfer from a vertical plate by free convection, MS thesis. Purdue University (1954)
8. Fujii, T.; Fujii, M.: The dependence of local Nusselt number on Prandtl number in the case of free convection along a vertical surface with uniform heat flux. Int. J. Heat Mass Transf. **19**, 121–122 (1976)
9. Churchill, S.W.; Ozoe, H.: A correlation for laminar free convection from a vertical plate. J. Heat Transf. **95**(4), 540–541 (1973)
10. Aydın, O.; Guessous, L.: Fundamental correlations for laminar and turbulent free convection from a uniformly heated vertical plate. Int. J. Heat Mass Transf. **44**, 4605–4611 (2001)
11. Kobus, C.J.; Guessous, L.; Raiker, V.: Modeling natural convection heat transfer from a uniformly heated vertical plate. Paper no. IMECE2003-42754, pp. 363–368 (2003)
12. Laein, R.P.; Rashidi, S.; Abolfazli Edfahani, J.: Experimental investigation of nanofluid free convection over the vertical and horizontal flat plates with uniform heat flux by PIV. Adv. Powder Technol. **27**, 312–322 (2016)
13. Fahiminia, M.; Naserian, M.M.; Goshayeshi, H.R.; Majidian, D.: Investigation of natural convection heat transfer coefficient on extended vertical base plates. Energy Power Eng. **3**, 174–180 (2011)
14. Saha, S.C.; Brown, R.J.; Gu, Y.T.: Scaling for the Prandtl number of the natural convection boundary layer of an inclined flat plate under uniform surface heat flux. Int. J. Heat Mass Transf. **55**, 2394–2401 (2012)
15. Teymourtash, A.R.; Khonakdar, D.R.; Raveshi, M.R.: Natural convection on a vertical plate with variable heat flux in supercritical fluids. J. Supercrit. Fluids **74**, 115–127 (2013)
16. Pantokratoras, A.: Laminar free-convection in glycerol with variable physical properties adjacent to a vertical plate with uniform heat flux. Int. J. Heat Mass Transf. **46**, 1675–1678 (2003)
17. Zitzmann, T.; Cook, M.; Pfrommer, P.: Simulation of steady-state natural convection using CFD. In: Ninth International IBPSA Conference, Montreal, Canada, pp. 1449–1456 (2005)
18. Khan, W.A.; Aziz, A.: Natural convection flow of a nanofluid over a vertical plate with uniform surface heat flux. Int. J. Thermal Sci. **50**, 1207–1214 (2011)
19. Perovic, B.D.; Klimenta, J.L.; Tasic, D.S.; Peuteman, J.L.G.; Klimenta, D.O.; Andjelkovic, L.N.: Modeling the effect of the inclination angle on natural convection from a flat plate, the case of a photovoltaic module. Thermal Sci. **21**, 925–938 (2017)
20. Guha, A.; Pradhan, K.: A unified integral theory of laminar natural convection over surfaces at arbitrary inclination from horizontal to vertical. Int. J. Thermal Sci. **111**, 475–490 (2017)
21. Bejan, A.: Convection Heat Transfer, pp. 112–113. Wiley, New York (1984)
22. Bouafia, M.; Hamimid, S.; Guellal, M.: Non-Boussinesq convection in a square cavity with surface thermal radiation. Int. J. Thermal Sci. **96**, 236–247 (2015)
23. Huang, J.; Stern, F.: A method to compute ship exhaust plumes with waves and wind. Int. J. Numer. Meth. Fluids (2010). https://doi.org/10.1002/fld